

Supporting Information

Multivalent nanobody engineering for enhanced physisorption and functional display on gold nanoparticles

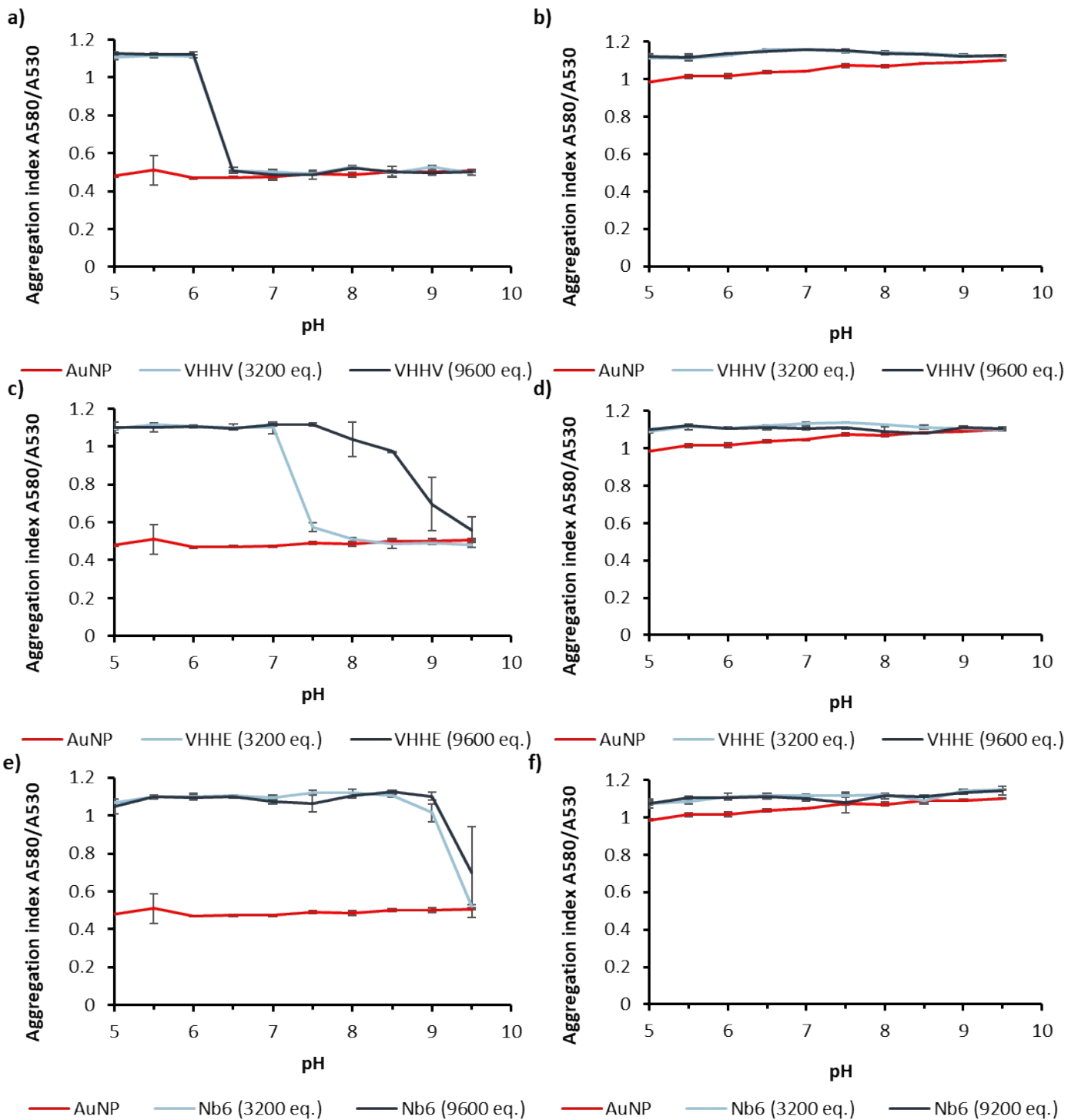
John-Paul Ayrton, Chapman Ho, Haoran Zhang, Vijay Chudasama, Stefanie Frank and Michael R Thomas

Supplementary table

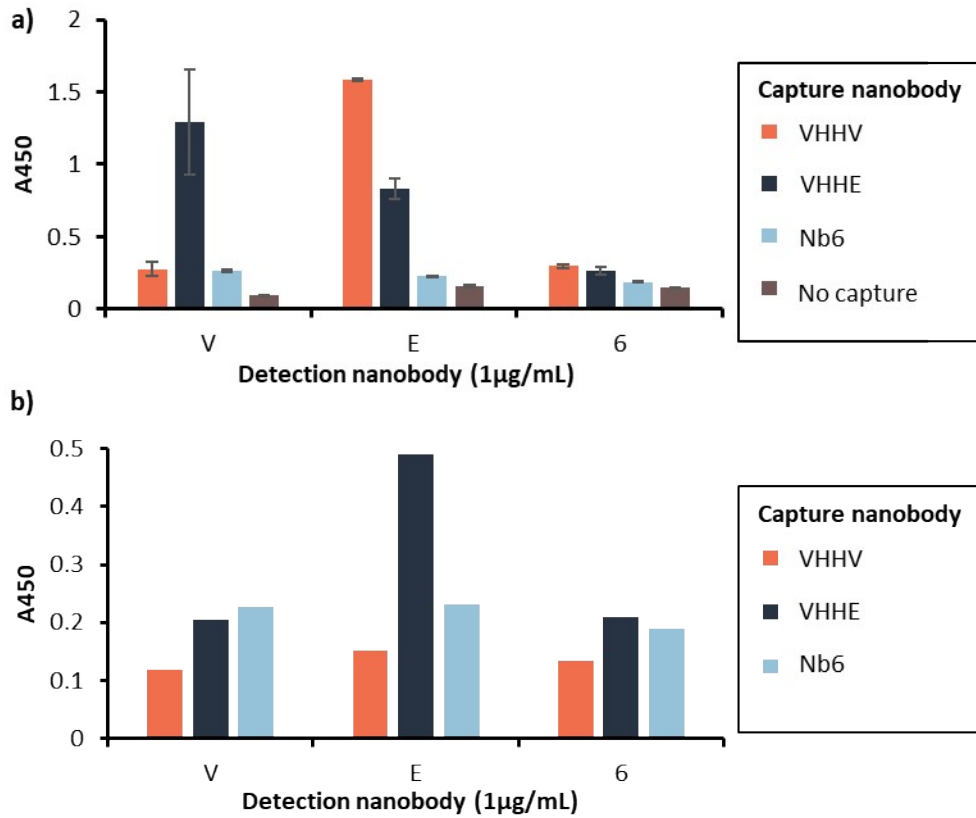
Nanobody	Amino acid sequence	MW (Da)
VHHV	MGQVQLVETGGGLVQPGGSLRLSCAASGFTFSSYAMGWARQVPG KGLEWVSYIYSDGSTYQDSVKGRFTISRDNASTVYLQMNSLKPE DTAVYYCATEGSLGGWGRDFGWSWGQGTQVTVSSLEHHHHHHH	14225.70
VHHE	MGQVQLVETGGGFVQPGGSLRLSCAASGVTLDYYAIGWFRQAPG KREGVSCIGSSDGRTYYSVSVKGRFTISRDNASTVYLQMNSLKPE EDTAVYYCALTVGTYYSGNYHYTCSDMDYWGKGTLLTVSSLEH HHHHH	15335.96
Nb6	MGQVQLVESGGGLVQAGGSLRLSCAASGIFGRNAMGWYRQAPG KERELVAGITRRGSITYYADSVKGRFTISRDNASTVYLQMNSLKPE EDTAVYYCAADPASPAPGDYWGQGTQVTVSSLEHHHHHHH	13937.58
VHHV-Cys	MGQVQLVETGGGLVQPGGSLRLSCAASGFTFSSYAMGWARQVPG KGLEWVSYIYSDGSTYQDSVKGRFTISRDNASTVYLQMNSLKPE DTAVYYCATEGSLGGWGRDFGWSWGQGTQVTVSSLEHHHHHHHC	14328.83
Cys-VHHV	CMGQVQLVETGGGLVQPGGSLRLSCAASGFTFSSYAMGWARQVP GKGLEWVSYIYSDGSTYQDSVKGRFTISRDNASTVYLQMNSLKPE EDTAVYYCATEGSLGGWGRDFGWSWGQGTQVTVSSLEHHHHHHH	14328.83
VHHV2	MGQVQLVETGGGLVQPGGSLRLSCAASGFTFSSYAMGWARQVPG KGLEWVSYIYSDGSTYQDSVKGRFTISRDNASTVYLQMNSLKPE DTAVYYCATEGSLGGWGRDFGWSWGQGTQVTVSSGGGGSGGGGS GGGGSQVQLVETGGGLVQPGGSLRLSCAASGFTFSSYAMGWARQ VPGKGLEWVSYIYSDGSTYQDSVKGRFTISRDNASTVYLQMNSL KPEDTAVYYCATEGSLGGWGRDFGWSWGQGTQVTVSSLEHHHHHHH	28125.87
VHHV3	MGQVQLVETGGGLVQPGGSLRLSCAASGFTFSSYAMGWARQVPG KGLEWVSYIYSDGSTYQDSVKGRFTISRDNASTVYLQMNSLKPE DTAVYYCATEGSLGGWGRDFGWSWGQGTQVTVSSGGGGSGGGGS GGGGSQVQLVETGGGLVQPGGSLRLSCAASGFTFSSYAMGWARQ VPGKGLEWVSYIYSDGSTYQDSVKGRFTISRDNASTVYLQMNSL KPEDTAVYYCATEGSLGGWGRDFGWSWGQGTQVTVSSGGGGSGGG GSGGGGSQVQLVETGGGLVQPGGSLRLSCAASGFTFSSYAMGWA RQVPGKGLEWVSYIYSDGSTYQDSVKGRFTISRDNASTVYLQM NSLKPEDTAVYYCATEGSLGGWGRDFGWSWGQGTQVTVSSLEHHH HHH	42026.04

Supplementary Table 1. Amino acid sequences and calculated mw for monovalent, cys-bearing and multivalent nanobodies.

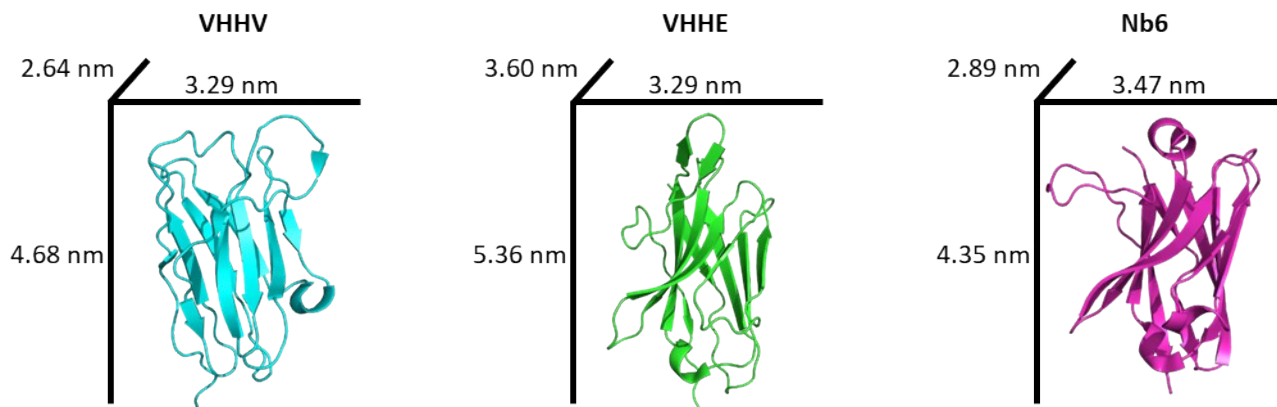
Supplementary figures



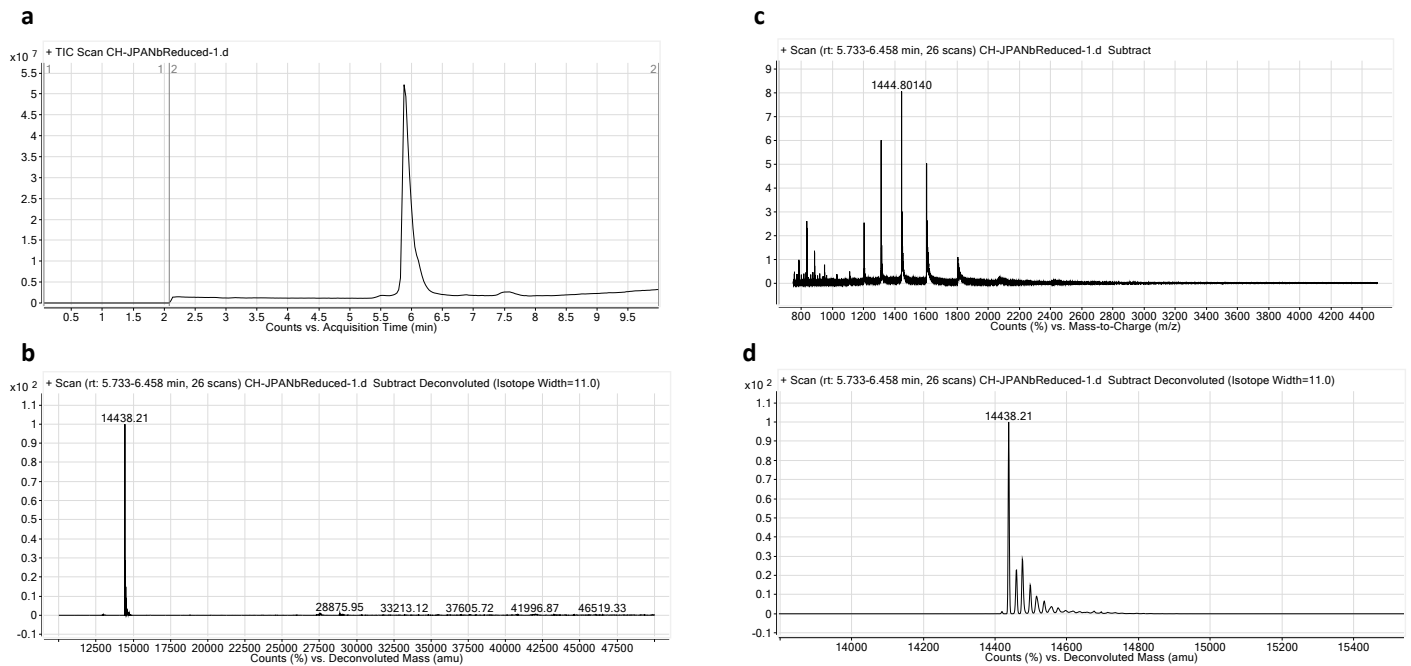
Supplementary Figure 1. Aggregation index plots of nanobody bioconjugations to 40nm AuNPs at a range of pH conditions (5.0 – 9.5) before and after increasing ionic strength (400mM NaCl) for nanobodies VHHV (a, b), VHHE (c, d), Nb6 (e, f). each nanobody was conjugated at 3200- or 9600-fold excess of nanobody to AuNP. Values are shown as average (n=3, VHHE at 9600-fold excess n= 2), and error bars indicate the standard deviation of the mean.



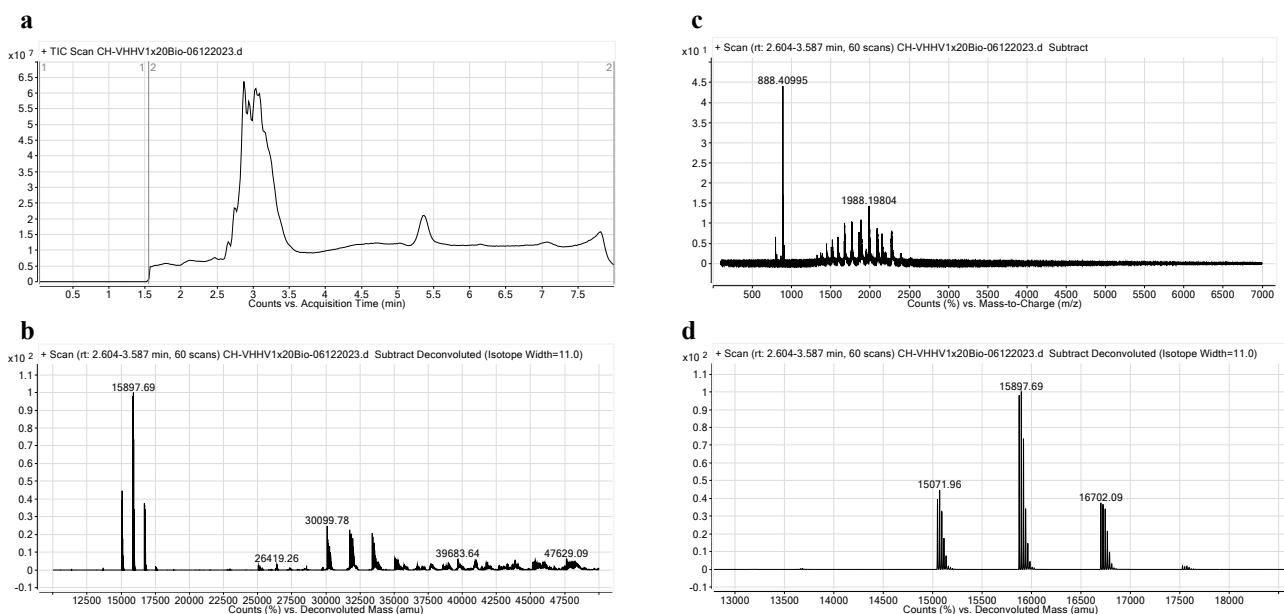
Supplementary Figure 2. Sandwich ELISA assessing the binding of SARS-CoV-2 RBD using paired nanobodies (VHHV, VHHE, and Nb6) as capture and detection reagents. **(a)** Signal intensity in the presence of 1 µg/mL RBD, shown as mean (n=2) ± standard deviation. **(b)** Control experiment with no RBD (n=1)



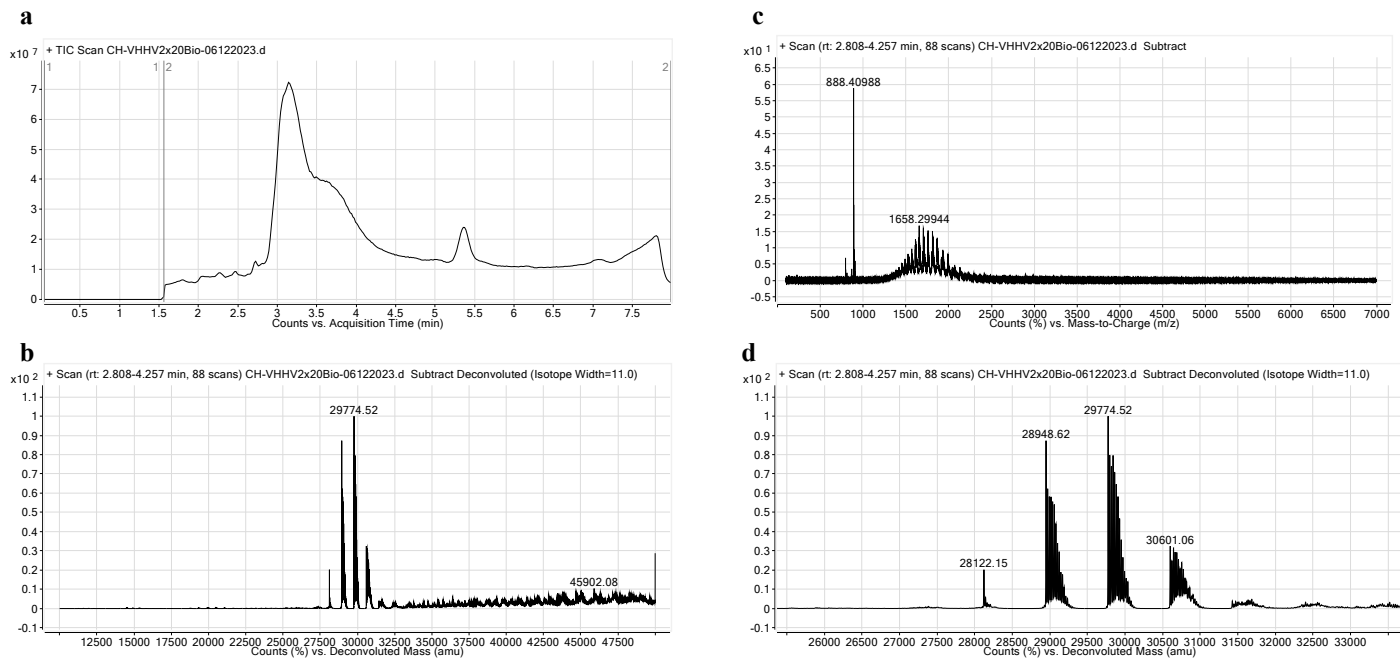
Supplementary Figure 3. Atomic reconstructions of Nanobodies VHHV (PDB ID: 7B18), VHHE (PDB ID: 7B14) and Nb6 (PDB ID: 7KKK) depicting the dimensions of each nanobody. The actual size of each nanobody is expected to be slightly larger due to the addition of flanking amino acids MG, LE and HHHHHH but this is not expected to have significant changes to interpretation of the DLS data.



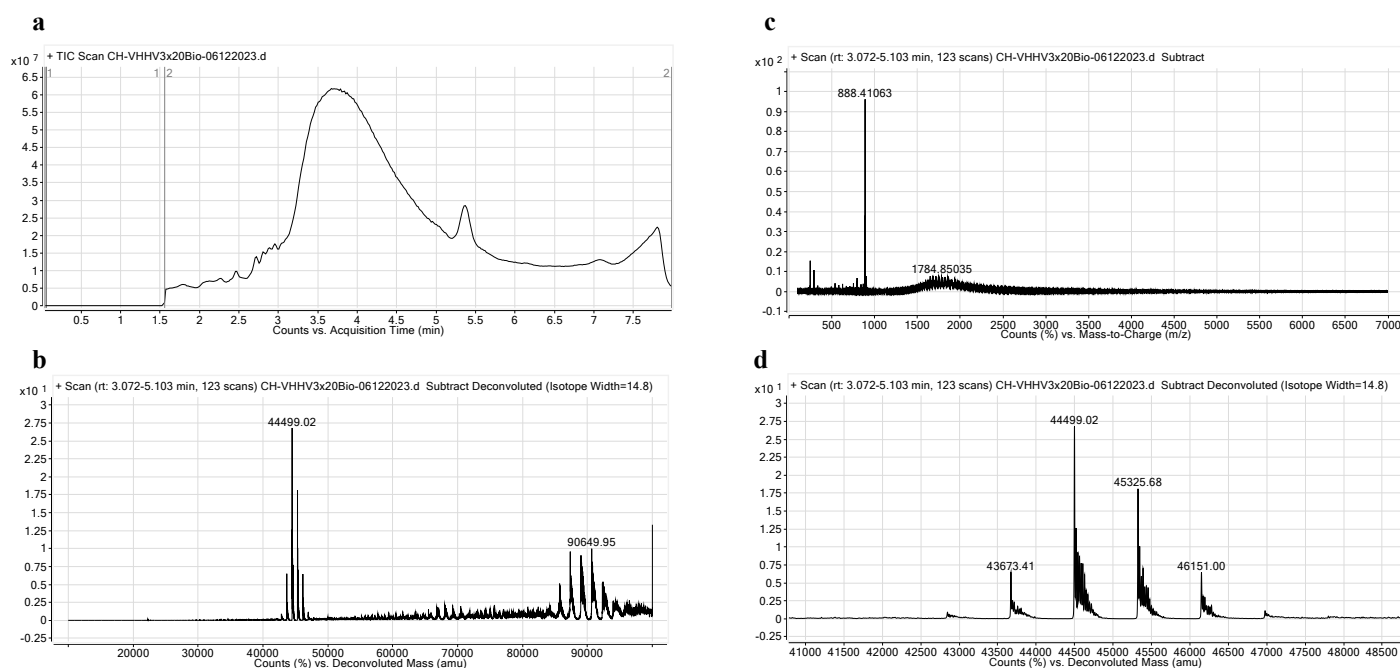
Supplementary Figure 4. LCMS spectra for VHHV-Cys after reduction with 10 mM TCEP, desalting, and reaction with N-Methylmaleimide (NMM) using LCMS. The addition of one NMM molecule (111.1 g/mol) to VHHV-Cys (14328.83 g/mol) was observed. **a** total ion chromatogram; **b** non-deconvoluted ion series mass spectrum; **c** deconvoluted ion series mass spectrum; **d** mass spectrum region of interest; observed mass 14438 corresponds to 1 NMM addition to reduced VHHV-Cys. The absence of a peak at 28657.3 g/mol indicates the complete reduction of the intermolecular disulfide bond, breaking the dimers into monomers. Additionally, the absence of peaks at 14,551.03 g/mol and 14,439.93 g/mol confirms that the internal disulfide bond remained intact. Reduction of this bond would enable the reaction of multiple NMM molecules per nanobody.



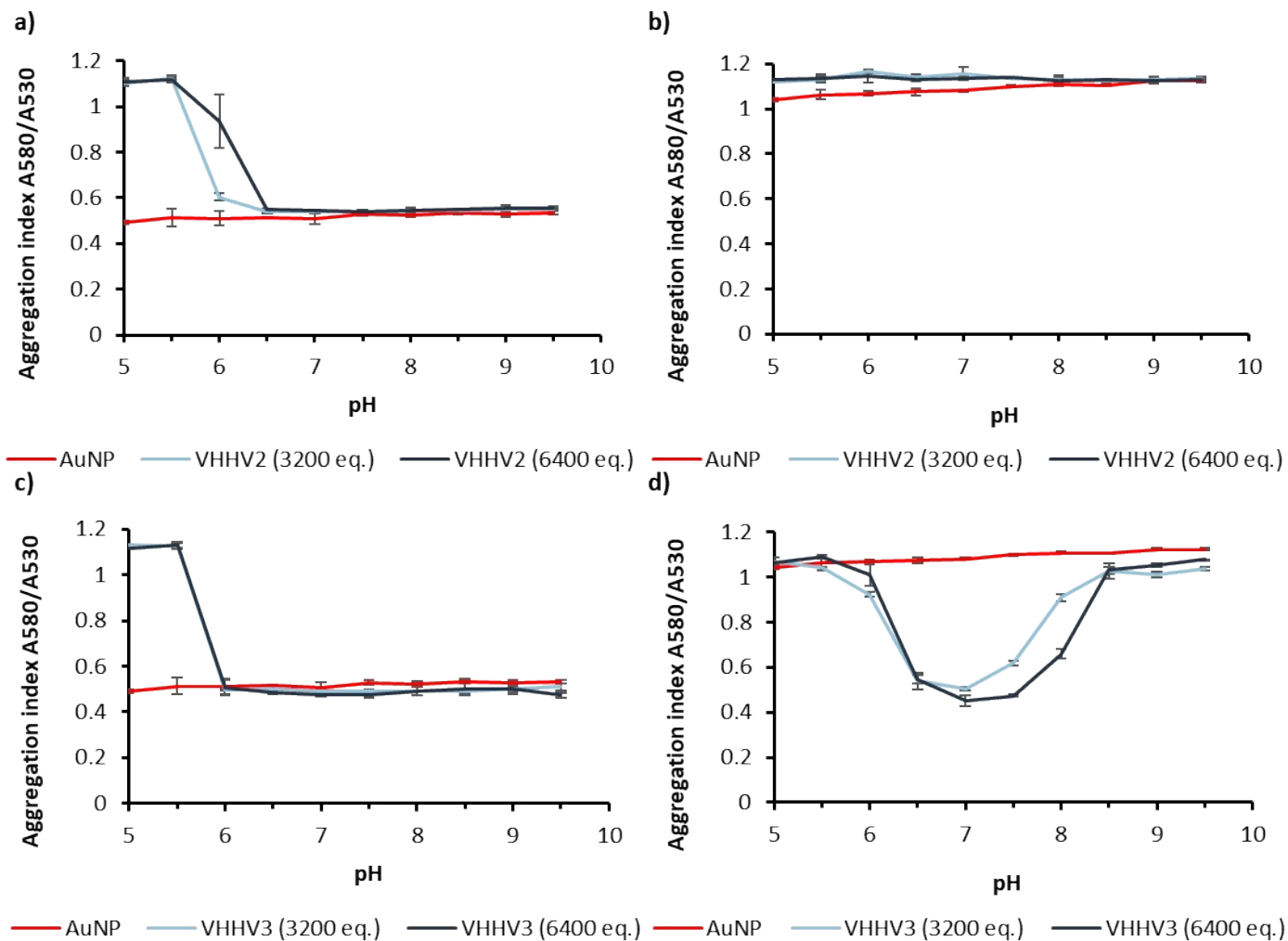
Supplementary Figure 5. LCMS spectra for VHHV-biotin conjugates showing the addition of NHS-PEG₁₂-Biotin (941.09 g/mol) to VHHV (14225.70 g/mol) with an expected increase in molecular weight of 825.64 g/mol per NHS-PEG₁₂-Biotin. **a** total ion chromatogram; **b** non-deconvoluted ion series mass spectrum; **c** deconvoluted ion series mass spectrum; **d** mass spectrum region of interest. Observed masses of 15071.96, 15897.69 and 16702.09 correspond to 1, 2 and 3 NHS-PEG₁₂-Biotin additions to VHHV nanobody respectively.



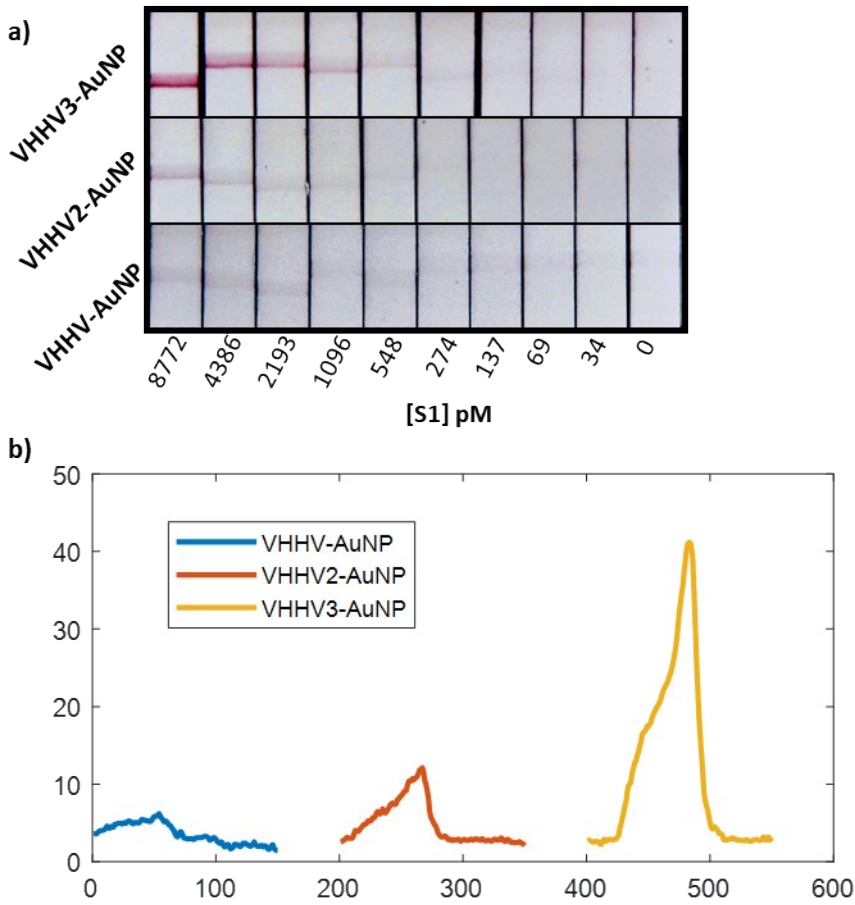
Supplementary Figure 6. LCMS spectra for VHHV2-biotin conjugates showing the addition of NHS-PEG₁₂-Biotin (941.09 g/mol) to VHHV2 (28125.87 g/mol) with an expected increase in molecular weight of 825.64 g/mol per NHS-PEG₁₂-Biotin. **a** total ion chromatogram; **b** non-deconvoluted ion series; **c** deconvoluted ion series mass spectrum; **d** mass spectrum region of interest. Observed masses of 28948.62, 29774.52 and 30601.06 correspond to 1, 2 and 3 NHS-PEG₁₂-biotin additions to VHHV2 nanobody respectively. Observed mass of 28122.15 corresponds to the unmodified VHHV2 nanobody.



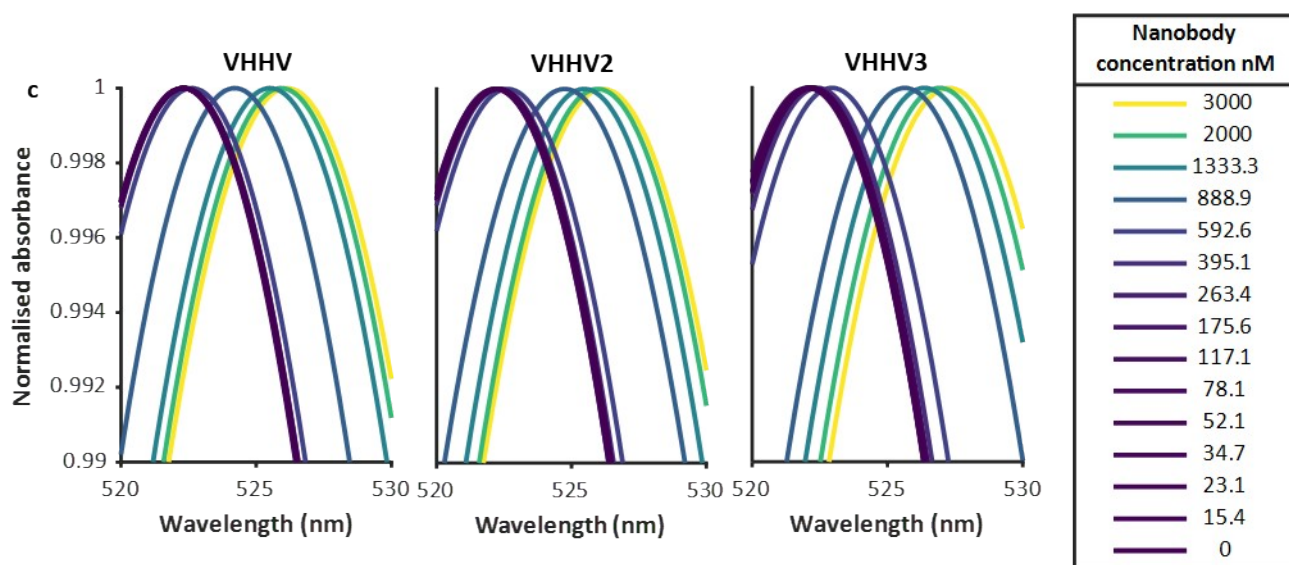
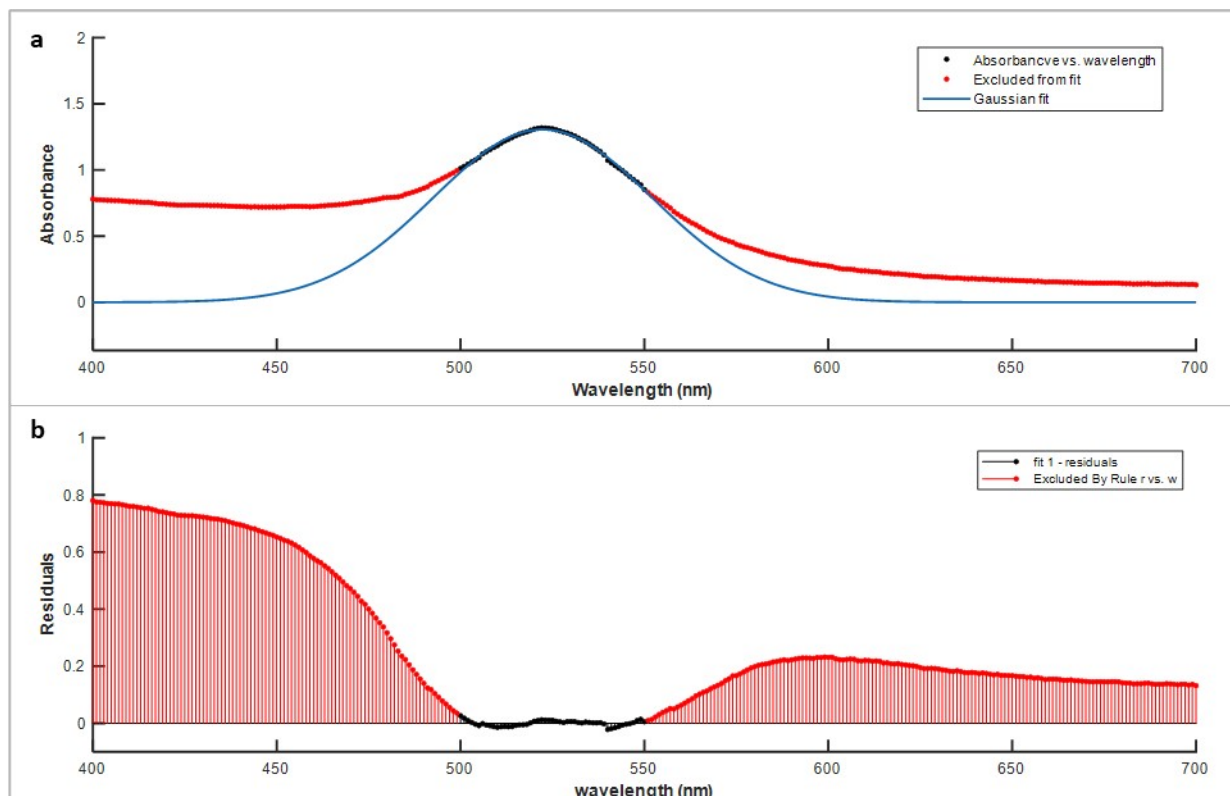
Supplementary Figure 7. LCMS spectra for VHHV3-biotin conjugates showing the addition of NHS-PEG₁₂-Biotin (941.09 g/mol) to VHHV3 (42026.04 g/mol) with an expected increase in molecular weight of 825.64 g/mol per NHS-PEG₁₂-Biotin. **a** total ion chromatogram; **b** non-deconvoluted ion series; **c** deconvoluted ion series mass spectrum; **d** mass spectrum region of interest. Observed masses of 43673.41, 44499.02, 45325.68 and 46151.00 correspond to 2, 3, 4 and 5 NHS-PEG₁₂-biotin additions to VHHV3 nanobody respectively.



Supplementary Figure 8. Aggregation index plots of nanobody bioconjugations to 40nm AuNPs at a range of pH conditions (5.0 – 9.5) before and after increasing ionic strength (400mM NaCl) for nanobodies VHHV2 (**a, b**), VHH3 (**c, d**). Each nanobody was conjugated at 3200- or 6400-fold excess of nanobody to AuNP. Values are shown as average (n=3) and error bars indicate the standard deviation of the mean.



Supplementary Figure 9 a) image enhanced lateral flow assay images to show the generation of signal at dilute antigen concentrations and the generation of nonspecific signal on the blank of VHHV-AuNP. b) test-line signal intensity profiles at high antigen at 8772pM of S1 protein.



Supplementary Figure 10. LSPR wavelength extraction. **(a)** Gaussian function fit to the UV-Vis spectrum of nanobody-AuNP bioconjugates from 500 to 550 nm. **(b)** residuals plot of the gaussian fit vs the data. **(c)** Plots of the fitted data across different concentrations of nanobodies for VHHV, VHHV2 and VHHV3.

Supplementary methods

Sandwich ELISA was performed by immobilizing monovalent nanobodies (VHHV, VHHE, or Nb66) onto high-binding plates at 1 $\mu\text{g}/\text{mL}$ in PBS overnight. The plates were washed with wash buffer, blocked with blocking buffer, and washed again. Then, 100 μL of either 1 $\mu\text{g}/\text{mL}$ or 0 $\mu\text{g}/\text{mL}$ of RBD in PBS was added to each well and incubated for 1 hour at room temperature with rocking. After washing, 100 μL of biotinylated detector nanobodies was added to each well and incubated for 1 hour. Following a wash step, 100 μL of streptavidin-HRP (SA-HRP) conjugate was added and incubated for another hour. After a final wash, 100 μL of TMB substrate was added, and the reaction was stopped with 2 M H_2SO_4 . The absorbance at 450 nm was measured to determine signal intensity.